Red Antenna States of Photosystem I from *Synechocystis* PCC 6803[†]

Marc Brecht,* Volker Radics, Jana B. Nieder, Hauke Studier, and Robert Bittl

Fachbereich Physik, Freie Universita¨t Berlin, Arnimalle 14, 14195 Berlin, Germany

Received January 22, 2008; Revised Manuscript Received March 20, 2008

ABSTRACT: Single-molecule spectroscopy at low temperatures was used to elucidate spectral properties, heterogeneities, and dynamics of the red-shifted chlorophyll *a* (Chl*a*) molecules responsible for the fluorescence from photosystem I (PSI). Emission spectra of single PSI complexes from the cyanobacterium *Synechocystis* PCC 6803 show zero-phonon lines (ZPLs) as well as broad intensity distributions without ZPLs. ZPLs are found most frequently on the blue side of the broad intensity distributions. The abundance of ZPLs decreases almost linearly at longer wavelengths. The distribution of ZPLs indicates the existence of at least two pools with maxima at 699 and 710 nm. The pool with the maximum at 710 nm is assigned to chlorophylls absorbing around 706 nm (C706), whereas the pool with the maximum at 699 nm (F699) can be assigned to chlorophylls absorbing at 692, 695, or 699 nm. The broad distributions dominating the red side of the spectra are made up of a low number of emitters assigned to the red-most pool C714. The properties of F699 show close relation to those of F698 in *Synechococcus* PCC 7002 and C708 in *Thermosynechococcus elongatus*. Furthermore, a high similarity is found between the C714 pool in *Synechocystis* PCC 6803 and C708 in *Synechococcus* PCC 7002 as well as C719 in *T. elongatus*.

Two transmembrane pigment−protein complexes, photosystem I (PSI)[1] and photosystem II (PSII), are essential for the light-driven oxygenic photosynthesis. This study focuses on PSI which transports, after photoexcitation, electrons from reduced plastocyanin or cytochrome c_6 on the luminal side to ferredoxin on the stromal side of the photosynthetic membrane (*1*). The first step of the light reaction is the absorption of a photon in the antenna system of PSI with subsequent energy transfer to the reaction center. At this point the captured excitation energy is used to induce a transmembrane charge separation starting from a pigment with main absorption at 700 nm (P700) (*1*−*3*). The absorption spectra of PSI from green plants, algae, and cyanobacteria show the existence of chlorophyll *a* (Chl*a*) molecules absorbing at lower energy than the usual Q_y absorption at 680 nm of Chl*a* in solution and, in particular, at lower excitation energy than the primary donor P700. These red-shifted Chl*a*s are often called the "red pools" or the "red-most" chlorophylls [for a review, see Gobets et al. (*4*) and Karapetyan et al. (*5*)]. Due to their spectral properties, Chl*a* dimers have been discussed as candidates for the red-pool Chl*a*s (see, e.g., refs *6*−*8*). If the excitation energy is localized within this "red-pool" Chl*a*, the stored energy is no longer sufficient to directly excite P700 to P700*. Additional activation energy, e.g., thermal energy of the phonon bath, is necessary to excite P700 and start the charge separation process. The question concerning the origin of the red shift and the physiological role of the red pool is puzzling (*9*−*11*). Even though the PSI complex from cyanobacteria differs in organization and polypeptide content to higher plants (*12*) and algae, the composition of the core structure of PSI from cyanobacteria and plants shows high similarity (*13*). Therefore, PSI from cyanobacteria is used to investigate key properties of all types of PSI. The well-resolved structural model for the cyanobacterium *Thermosynechococcus elongatus* (*T. elongatus*, previously *Synechococcus elongatus*) from X-ray crystallography (*14*−*16*) is used as a reference structure for PSI in general. For PSI from *T. elongatus* four red pools with different spectroscopic properties were found. They were called C708, C715, C719, and C735 according to their proposed mean absorption wavelength. Two of those pools (C708 and C719) were identified by absorption (*17*), one by hole-burning spectroscopy (C715) (*18*), and one (C735) (*19*) by single-molecule spectroscopy (SMS).

The red absorption in PSI from *Synechocystis* PCC 6803 at low temperature consists of a single band centered at 708 nm (*20*). With hole-burning spectroscopy it was shown that the red side of this absorption band shows much stronger electron−phonon coupling than the blue side, suggesting that there are (at least) two states underlying the absorption (*18, 21*−*23*). These two states were named C706 and C714, due to their mean absorption wavelength at 706 and 714 nm, respectively. Both show large inhomogeneous broadening and remarkable spectral overlap. Stark hole-burning spectra on PSI (*24*) suggest a large heterogeneity of the induced dipole moment changes in the close vicinity of the responsible chromophores (*18*) or large variations of the inherent dipole moment change of the Chl*a* species (*22*). The low-temperature fluorescence spectrum of *Synechocystis* PCC

[†] This work was supported by Volkswagenstiftung in the framework of the program: Physics, chemistry and biology with single molecules (I/78361).

* To whom correspondence should be addressed: e-mail, brecht@hydrogenase.de; phone, ++49-30-838-56047; fax, ++49-30-838-56046.

[1] Abbreviations: PSI, photosystem I; Chl*a*, chlorophyll *a*; SMS, single-molecule spectroscopy; ZPL, zero-phonon line; PW, phonon wing.

10.1021/bi800121t CCC: $40.75
Published on Web 04/23/2008

6803 is characterized by a broad contribution peaking at 718.5 nm (*20*). The anisotropy of the emission depends strongly on the excitation wavelength. Excitation at 693.5 nm yields an almost complete depolarization of the emission for wavelengths longer than 718.5 nm, whereas excitation at and above 705.5 nm yields a value for the anisotropy close to the theoretical maximum over the whole range of the emission. This indicates that either there is no energy transfer between the remaining red-shifted chlorophylls or the transfer occurs between emitters with almost parallel Q_y transitions (*20*).

Due to the unstructured shape of the bulk fluorescence spectra it remains difficult to obtain detailed information about the spectral characteristics of the red Chl*a*s. This drawback can be avoided by single-molecule spectroscopy (SMS) (*25*). SMS overcomes ensemble averaging completely, and the fluorescence emission of single chromophores becomes accessible (*26*). The observation of single chromophores yields spectral characteristics that are hidden by ensemble averaging. For example, at low temperature these are a narrow zero-phonon line (ZPL) and a broad phonon wing (PW). The ZPL belongs to an electronic transition without phonon creation (lattice vibrational modes) or annihilation. The PW on the low-energy side of the ZPL is due to the interaction of the chromophore with its surrounding leading to the excitation of phonons. Relative to the ZPL the maximum of the PW is shifted to the red by 20−30 cm^{-1} and has a width of ∼30 cm^{-1} in proteins (*27*).

SMS on PSI from *T. elongatus* and *Synechococcus* PCC 7002 at cryogenic temperature showed sharp emission lines and a broad unstructured intensity distribution. This broad intensity with typically more than 10 nm red shift relative to the ZPLs cannot be identified as the PWs of the ZPLs. For PSI from *T. elongatus* the sharp ZPLs in the range below 717 nm can be assigned to emitters absorbing around 708 nm (C708), whereas the broad intensity distributions can be assigned to more red-shifted Chl*a*s around 719 nm (C719) (*28, 29*). For PSI from *Synechococcus* PCC 7002 sharp ZPLs were found below 710 nm; their distribution shows a maximum at 698 nm (F698), and the broad intensity distributions were assigned to the red-most pool absorbing at 708 nm (C708) (*30*). The emitters showing sharp ZPLs are subject to spectral diffusion changing their emission frequency with rates lower than the acquisition time of the single spectra, whereas the emitters of the broad intensity distributions undergo a much faster spectral diffusion, yielding a complete broadening of the ZPLs within the acquisition time of a single spectrum.

In this contribution we show single-molecule spectra of PSI from *Synechocystis* PCC 6803. The spectra taken with short accumulation time show sharp ZPLs that spread over a wide spectral range. These ZPLs show a time-dependent line broadening. The analysis of the spectra yields at minimum three pools, F699, C706, and C714, contributing to the fluorescence emission. Their properties resemble those observed for Chl*a* pools in PSI from *T. elongatus* and *Synechococcus* PCC 7002. On the basis of this information a tentative assignment to Chl*a* in the X-ray structure of PSI is discussed.

MATERIALS AND METHODS

PSI from the *Synechocystis* PCC 6803 has been isolated as described in ref *31*. Purified PSI trimers were at first diluted in buffer at pH 7.5 containing 20 mM Tricine, 25 mM $MgCl_2$, and 0.4 mM (0.02% w/v) detergent (β-DM; Sigma) to reach a concentration of about 20 μM Chl*a*. This amount of detergent is adequate for the critical solubilization concentration for a PSI trimer concentration of 0.5 μM, avoiding PSI aggregation (*32*). For prereduction of P700 5 mM sodium ascorbate was added. In further steps this PSI-containing solution was diluted to a PSI trimer concentration of 3 pM. Less than 1 μL of this sample was placed between two coverslips, assuring spatial separation of individual PSI trimers. Sample preparation and mounting were accomplished under indirect daylight. We used a home-built confocal microscope to observe the fluorescence emission of single molecules; the experimental setup was described recently in ref *29*. The sample and the microscope objective were immersed in superfluid He, and the sample temperature was 1.4 K during all experiments. Such cryogenic temperatures are a prerequisite for detecting narrow ZPLs. The excitation power measured directly behind the beam-scanning module was 100 μW, and the excitation wavelength was 680 nm for all spectra.

RESULTS

Emission Spectra of Individual Complexes. Single PSI complexes can be detected at low temperature using the fluorescence emission of the red Chl*a* (*28*). At low temperature these Chl*a* molecules act as traps for the excitation energy and have a significant fluorescence quantum yield. Figure 1 shows the average spectrum (on top) obtained from the summation of the fluorescence emission spectra from 100 single PSI complexes from *Synechocystis* PCC 6803 as well as a selection of five fluorescence emission spectra (denoted I−V) of different single PSI complexes. The acquisition time for the spectra from the single complexes was 100 s. For better comparability, the spectra that exhibited intensity differences of ∼30% were scaled to a similar magnitude. Each spectrum exhibits unique features that will be described briefly. Spectrum I consists of a broad emission beginning with a steep increase of intensity at 700 nm and a smooth decay for λ >715 nm. In addition, a weak peak with low intensity at 699 nm as well as two clear peaks at 703.1 and 710.2 nm can be seen in this spectrum. We interpret these lines as broadened ZPLs (see below). Spectrum II shows also a broad intensity distribution with a steep intensity increase at the blue side, but the onset is shifted to 707 nm. The maximum of this distribution is found at ∼714 nm. At the blue side, between 704 and 708 nm, an additional broad intensity distribution with less intensity is visible. At the red end of the steep increase, at 711.0 nm, a small ZPL can be seen. Spectrum III shows also a broad intensity distribution. The increase of this distribution can be separated in two parts, one from 707 to 712 nm and the other from 712 to 715 nm. In the first part a steady intensity increase is observed that flattens toward 712 nm. In the second part a steep intensity increase follows that proceeds into the edge of an intense peak at 715.8 nm followed by a smooth intensity decrease. In spectrum IV, the emission of the PSI complex starts at 703.3 nm with a sharp ZPL followed by a region of almost

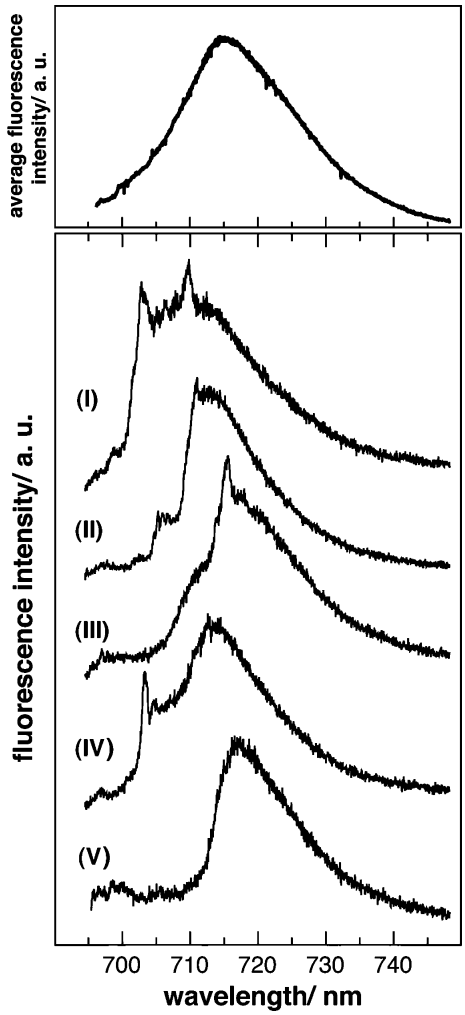

FIGURE 1: Single-molecule fluorescence emission spectra from PSI complexes of *Synechocystis* PCC 6803. Spectra were recorded on different individual complexes. The accumulation time was 100 s for each complex. The spectrum on top represents the average emission spectrum of the spectra from all 100 measured individual complexes. Excitation wavelength 680 nm; temperature 1.4 K.

constant intensity from 704 to 708 nm passing into a steady increase of the intensity toward the maximum of the intensity distribution at 714 nm. In the last spectrum, V, only a broad intensity distribution is found with maximum at 717.7 nm. The increase of intensity at the blue side is steeper than the smooth decay on the red side. The majority of fluorescence emission spectra recorded for single PSI complexes of *Synechocystis* PCC 6803 shows indications for ZPLs. In some spectra the ZPLs show up as intense narrow lines, and in some spectra they are observed as broad features. The intensity emitted by these ZPLs compared with the overall intensity remains small. The number of the ZPLs, their spectral position, and line width, γ, vary from complex to complex. In spectra taken within 100 s the line width ranges from ~0.5 nm to several nanometers.

Reducing the accumulation time affects the characteristics of the spectra remarkably. This is shown in Figure 2 for two series of spectra taken within 1, 20, and 150 s. These series stem from two different complexes showing rather extreme behavior. The spectra of the complex given in Figure 2a serve as an example for slow broadening of the ZPLs during time. The spectra show three ZPLs (at 696.2, 689.2, and 700.5 nm) and a broad intensity distribution centered around 716

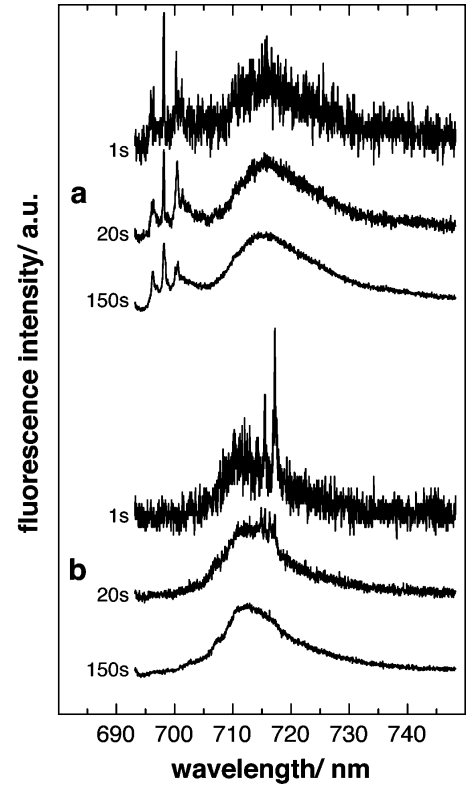

FIGURE 2: Dependence of fluorescence emission spectra of two different single PSI complexes on acquisition time. Excitation wavelength 680 nm; temperature 1.4 K.

nm. The increase of the accumulation time is accompanied by an increase of the line width of the three ZPLs. The line width fitted with a Gaussian line shape increases from the spectrum acquired within 1 s by a factor of 2, and four for the red-most and the blue-most ZPL in the spectrum accumulated for 150 s. The width of the broad emission around 716 nm remains unchanged by the increase of the accumulation time. The spectra of the complex given in Figure 2b serve as an example for a fast broadening of the ZPL in time. In the spectrum taken within 1 s clear ZPLs are visible at 715.5 and 717.3 nm. In the spectrum taken within 20 s these clear lines begin to disappear and are completely lost in the spectrum taken within 150 s accumulation time. In general, we observe an increase of the ZPL line width with the accumulation time.

Spectral Dynamics and Intensity Variations of ZPLs. The underlying dynamical processes leading to the spectral broadening can be analyzed in our setup with sufficient S/N ratio using an acquisition time of ~1 s. In order to analyze the spectral dynamics in the emission of PSI from *Synechocystis* PCC 6803 sequences of fluorescence spectra covering the whole spectral range were recorded for 100 complexes. In the following we focus on the dynamical behavior of the ZPLs within these spectra and, therefore, show only narrow sections for clarity. Two sequences showing representative examples of the dynamical behavior of the ZPLs are shown in Figure 3. The sequences consist of 120 spectra consecutively recorded with 1 s acquisition time. The sequence given on the left shows an example for a ZPL that resides for a long time within a narrow wavelength region. In the first 108 s this ZPL remains in a restricted wavelength region centered around 704.5 nm. During this time the line shivers within a range

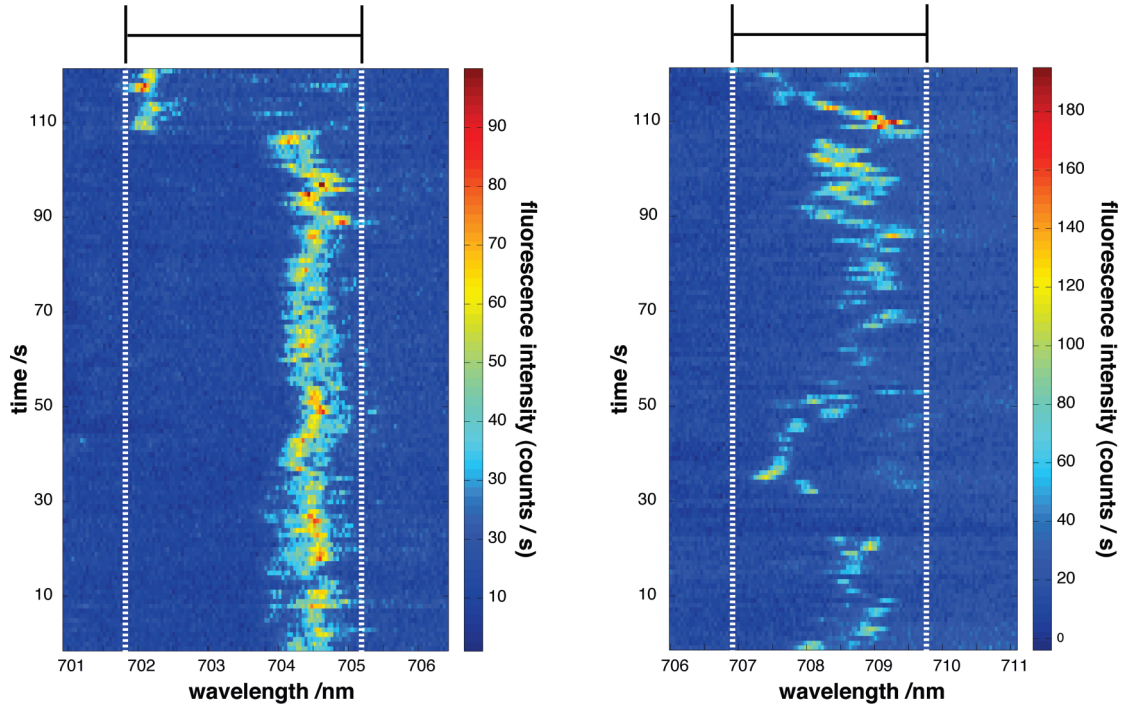

FIGURE 3: Plots of time-dependent fluorescence emission spectra of PSI. Sequence of spectra covering the individual wavelength range of the ZPLs for two different complexes are given. The time sequences of 120 spectra with an accumulation time of 1 s for each spectrum are displayed for both complexes. The vertical bars on the top of the trails indicate the areas given in Figure 4A (see also text). Excitation wavelength 680 nm; temperature 1.4 K.

of 0.6 nm around its mean position. After this period the ZPL makes a wide frequency jump of 2.5 nm to 702 nm. Thereafter, the ZPL remains at this new position and shivers similarly as before. The trail given on the right of Figure 3 shows an example for a ZPL changing its wavelength position remarkably with a high rate. The different spectral positions are occupied for durations close to the acquisition time of individual spectra. Two or more spectral positions can be observed in cases where the line resides on a spectral position shorter than the acquisition time. From the behavior of the ZPLs shown in the picture as well as all other observed ZPLs the existence of discrete spectral positions taken successively along the spectral trail is very likely. In addition to the variation of the spectral position, we observe also changes of the intensity of the ZPL. Such intensity fluctuations can be seen in both sequences shown in Figure 3. This is most obvious in the right sequence where the ZPL disappears after the first 23 s for 7 s and then reappears again. Overall, the ZPLs show dynamical variations of their spectral positions and their intensity. These variations differ from complex to complex, but, as a common feature, the ZPLs remain in restricted spectral areas. To illustrate such restricted areas white dashed lines representing their borders were included in Figure 3. For the left data set this area spans from 701.8 to 705 nm and for the right it spans from 707 to 709.5 nm. Bars on the top of each data set also indicate their width.

Spectral Distribution of ZPLs. The width and the spectral position of the restricted areas within the ZPLs can be found in the sequences of spectra from individual complexes determined for 100 complexes. A compilation of the results is given in Figure 4A. The determined areas are given for each complex individually by bars. The spectral ranges occupied by the spectral trails of the ZPLs are in some cases well separated, and in some cases they overlap. In the cases where well-separated spectral ranges were observed, the ranges represent the dynamical region of one single line. In the case of overlapping ranges, consequently, the ranges were combined to one joint broad range. The spectral areas covered by ZPLs vary by width and number for the different complexes. With only few exceptions between one and three separated ranges were determined. The average width of these areas is ~3.8 nm.

The number of molecules showing ZPLs at a specific wavelength was determined from Figure 4A and plotted in Figure 4B. It shows an almost monotonous decay from 697 to 722 nm. A minor deviation from monotony is found around the trough at 705 nm. At the blue side (around 700 nm) almost all PSI complexes show ZPLs; toward lower energies the number of observable ZPLs decreases. The observation of ZPLs at wavelengths larger than 722 nm remains an exception.

Assignment of Spectral Components. Two red pools, C706 and C714, are known for *Synechocystis* PCC 6803 so far (*18, 23*). Both pools were observed and characterized by hole-burning spectroscopy. The associated maxima of the fluorescence emission of C706 and C714 are expected at 710 and 722 nm, respectively. For both cases a width of ~15 nm was determined (*18, 23*). ZPLs in the range expected for C706 are abundant in our SMS data, whereas ZPLs in the range expected for C714 are scarce. In Figure 4B a Gaussian line was included using the expected maximum position and the line width for C706 (red curve). This curve is in good agreement with the number of ZPLs found above 705 nm. In order to also cover the ZPLs below 705 nm a second Gaussian with maximum position at 699 nm and a width of 7 nm has been included (orange curve). In

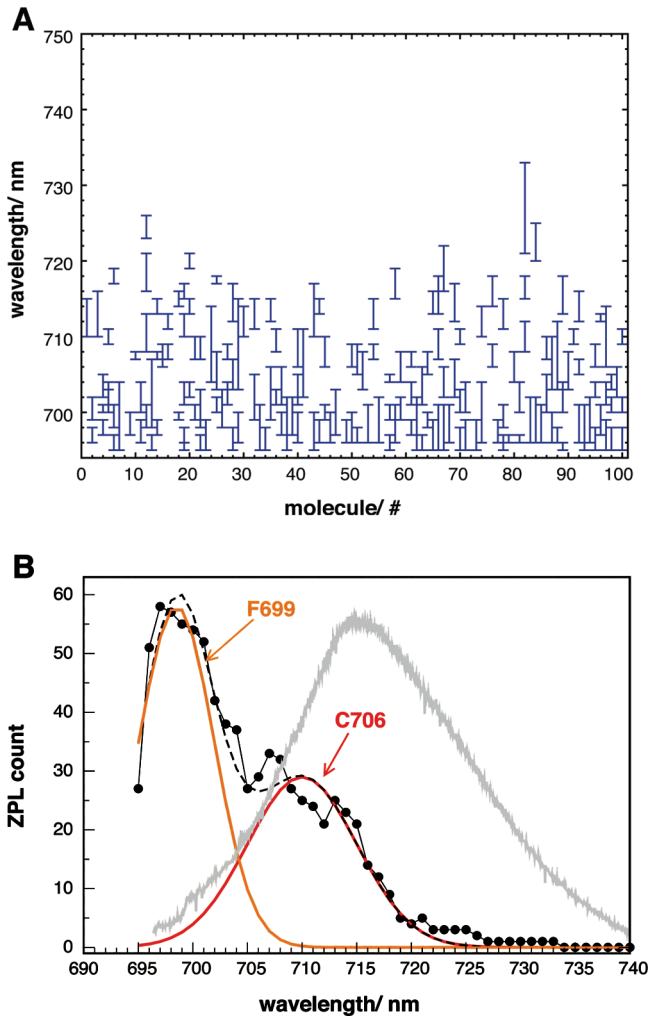

FIGURE 4: (A) Statistical analysis of the distribution of ZPLs. The chart shows the individual spectral regions in which the ZPLs were observed in the sequence of spectra of 100 PSI complexes. The determination of these areas from the sequences is explained in the text and visualized in Figure 3. (B) The number of molecules showing a ZPL at a given wavelength position is given by dots, representing the number of bars shown in panel A (bin size 1 nm). The distribution (- - -) is fitted with two Gaussians (orange, red); for details see also text. The gray curve represents the average spectrum from Figure 1.

conjunction with C706 a good agreement with the experimental finding (dashed curve) is archived. Due to the maximum position at 699 nm we introduce the abbreviation F699 for this pool.

The average fluorescence emission of all spectra from the top of Figure 1 was also included in Figure 4B (gray curve). The comparison between the average fluorescence emission and the distribution of the ZPLs shows that the ZPL distribution does not mirror the fluorescence intensity. The highest probability for observing a ZPL is found at the blue end of the spectra where the overall fluorescence emission almost vanishes. On the other hand, there is only a small probability to observe a ZPL at the maximum of the fluorescence intensity. Therefore, further emitting states contributing to the fluorescence emission must be present. The red shift of those states must be larger than the red shift for C706. Due to the spectral position it is most probable to associate these states with the pool C714 found by hole burning.

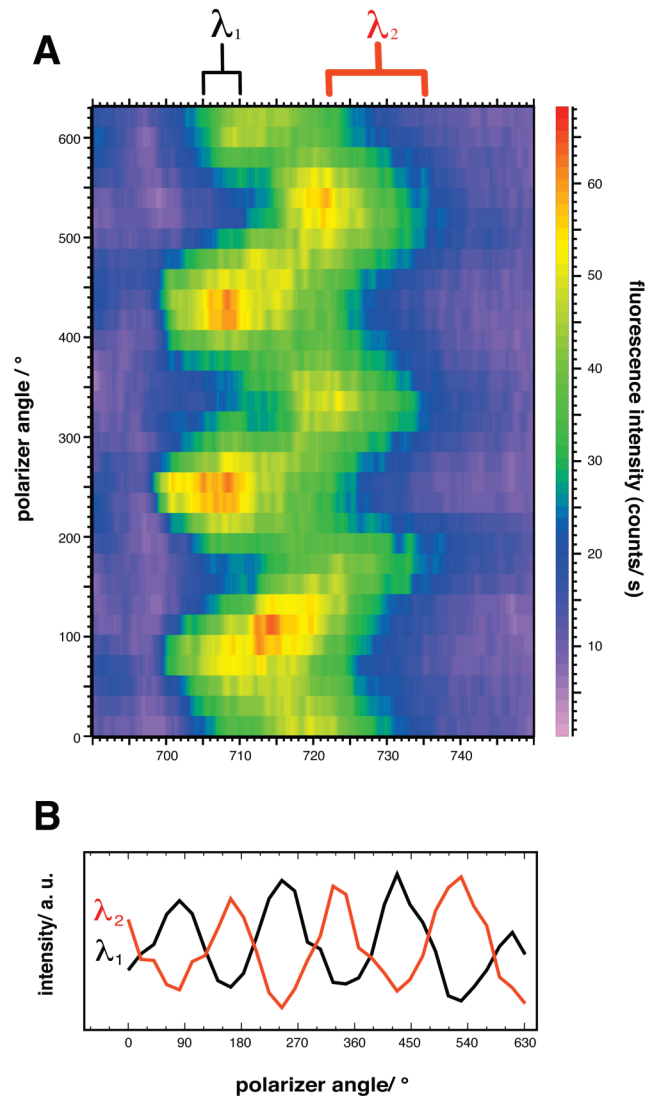

FIGURE 5: (A) Sequence of fluorescence emission spectra of a single PSI complex as a function of the orientation of the polarizer in front of the spectrograph. The acquisition time was 5 s for each spectrum. Excitation wavelength 680 nm; temperature 1.4 K. A complex of the type V from Figure 1 was chosen, i.e., showed no resolved ZPLs. The individual spectra were recorded in steps of 20°. The angle of the polarizer is shown on the left side. The fluorescence intensity is encoded in the color scale on the right. (B) Integrated fluorescence intensity of the emission of a single PSI complex in the range from 705 to 710 nm (λ_1) and 722 to 735 nm (λ_2) as a function of the polarizer angle.

Further details about the number and spectral positions of emitters responsible for the fluorescence emission of single PSI complexes are obtained from the analysis of their polarization. Figure 5 shows the emission from a single PSI complex in dependence of the polarizer angle in front of the spectrograph. This angle is defined with respect to an arbitrary laboratory axis and is uncorrelated to the polarization of the excitation light. In Figure 5A the dependence of the whole emission spectra as a function of the polarizer orientation is shown. Two pronounced contributions can be distinguished. The emission of these contributions is linearly polarized, approaching the dark count level at the minima. From this data set, the integrated fluorescence intensity was determined for the ranges 705−710 nm (λ_1) and 722−735 nm (λ_2) and is displayed in Figure 5B. In this representation a sinusoidal

shape of the curves with a periodicity of 180° can be seen. Similar strong polarization of emitters responsible for the fluorescence emission was observed for all PSI complexes investigated in this way. The emission found within λ_1 can be assigned to a member of C706 and the red emission within λ_2 is due to an emitting state of the pool C714. Due to the large inhomogeneous broadening of the pools, an assignment of emitters of one single complex always remains tentative. A strong polarization of the fluorescence emission from the different pools requires either a single emitter as the origin of the emission or a number of emitters with parallel transition dipole moments. Since the PSI complexes in our samples are randomly oriented, it is unlikely that the transition moments of several emitters would appear parallel in all cases.

DISCUSSION

Inhomogeneous Broadening and Spectral Jumps. The average emission spectrum of all single PSI complexes from *Synechocystis* PCC 6803 (Figure 1) is in good agreement with the spectral characteristics of bulk emission spectra (*20, 21*). Like the 4.2 K bulk fluorescence spectra (*20*), this average emission spectrum shows no indication of fluorescence other than the band with the maximum at 717.7 nm. The slight differences in the maximum position of the average single-molecule spectrum and the bulk emission spectrum are likely due to the different sample preparation conditions (see Materials and Methods).

The inhomogeneous broadening of the ensemble spectra can be lifted by SMS, and the fluorescence emission of single complexes can be observed. The SM spectra from *Synechocystis* PCC 6803 exhibit a distinct heterogeneity (Figure 1). Most of the SM spectra show a broad intensity distribution and indications for broadened ZPLs. The line width, spectral position, and the intensity of the observed ZPLs vary from complex to complex. Spectral diffusion was identified to be the main broadening process for those ZPLs (Figure 2). Even at low temperature (1.4 K) the emission of one chromophore is not fixed to a specific wavelength as has been shown for single bacterial light-harvesting complex 2 (LH2) by fluorescence excitation spectroscopy (*33*) and on single PSI complexes by fluorescence emission spectroscopy (*29, 30*). The transition energy of the observed ZPLs varies in both cases during time, yielding line jumps on the nanometer scale and line broadening processes. Recording of the sequence of spectra for single PSI complexes from *Synechocystis* PCC 6803 (Figure 3) shows that the spectral diffusion process originates from discrete spectral jumps of the ZPLs. The width of these jumps extend into the nanometer range. The rate of the jump processes often meets the range of our experimental time resolution (0.3−1 s). If the jump rate is faster than the experimental time resolution, one emitter gives rise to ZPLs at multiple wavelength positions in the spectra. However, multiple lines in one spectrum can also arise from different emitting states. Therefore, an unique explanation of the occurrence of multiple ZPLs within one spectrum is impossible. Jumps between different wavelength positions of a ZPL were interpreted as hopping between conformational substates in the energy landscape of a protein (*33, 34*).

Origin of the Spectral Pools F699, C706, and C714. The sequences of spectra of single molecules show that the individual observed ZPLs reside within limited spectral ranges. The width and the spectral position of those ranges can be extracted from the sequences (Figure 3). The collection of all of these confined areas (Figure 4) can be explained by at least two contributions, F699 and C706. The spectral ranges covered by F699 and C706 represent only a small portion of the overall fluorescence emission of PSI from *Synechocystis* PCC 6803. The ZPLs of the pool F699 may be due to the emission from one or more states seen in hole-burning spectra at 692, 695, or 699 nm (*23*). The properties of F699 visible on the single-molecule level show similarities with the emission of F698 from *Synechococcus* PCC 7002 and C708 from *T. elongatus*. These three pools give rise to well-resolved ZPLs with high abundance in the spectra. Their ZPLs show line jumps with similar rates and widths. On the basis of these spectroscopic similarities, it can be assumed that the chomophores and their close environment show structural equivalence.

The percentage of PSI complexes showing ZPLs decreases toward 720 nm. This is in contrast to the increase of the overall fluorescence emission intensity in that range (see Figure 4B). Therefore, a considerable amount of fluorescence emission from C706 is not accompanied by resolvable ZPLs. This tendency is even increased in the range of the expected emission of C714, where the largest amount of fluorescence is emitted and almost no ZPLs are observed, probably due to a faster spectral diffusion process preventing the detection of resolved ZPLs (see also below). Spectral diffusion may also explain the absence of ZPLs in the C706 range in single-molecule spectra recorded with longer accumulation times (*35*).

The dominating part of the fluorescence intensity is emitted in a broad intensity distribution. Such broad distributions are observed in almost all spectra (Figure 1). Due to their spectral position it is most reasonable to assign them to the emission of the pool C714. In many cases the width of these broad intensity distributions reaches the line width determined for the pool C714 (*18*). Fluorescence emission spectra taken with a rotating polarizer in front of the spectrograph indicate a high degree of polarization for the whole range of the emission (Figure 5). Thus, the number of emitters responsible for the broad intensity distribution has to be small. This in turn leads to the conclusion that the emitters of C714 are able to cover almost the complete inhomogeneous width even under cryogenic conditions. Observation of resolved ZPLs or even indications for ZPLs are scarce in the spectral region above 720 nm, in contrast to the expectation that each single emitter should consist of a ZPL and a PW. A similar observation occurred in the single-molecule experiments on C719 (*T. elongatus*) (*29*) and C708 (*Synechococcus* PCC 7002) (*30*). It was argued that a large electron−phonon coupling in conjunction with spectral diffusion can explain the absence of ZPLs in the spectra (*29*). The electron−phonon coupling determined by hole burning for C714 is close to the values found for C719 of *T. elongatus* (*18*), and strong spectral diffusion dominates C714, as can be seen by the fast disappearance of the ZPLs in Figure 4B. Therefore, both conditions leading to a loss of ZPLs are fulfilled for C714. Fast spectral diffusion over a large spectral range gives

indications for barriers in the energy landscape that can easily be crossed at the given low-temperature conditions. Compared to F699 and C706, the barriers for C714 must have reduced heights. Such a reduction of the heights corresponds to a flattening of the energy landscape. The chromophores and their environment have a composition allowing more flexibility. Due to this composition, the chromophores can change more easily to other conformational substates. This, in turn, implies that the chromophores of C714 have higher flexibility than the chromophores associated with F699 and C706.

Candidate Molecules for the Emitting States. Due to the lack of an X-ray structure for *Synechocystis* PCC 6803 an assignment attempt for the pools F699, C706, and C714 is not directly possible. Nevertheless, the sequence homology between PSI from *Synechocystis* PCC 6803 and *T. elongatus* allows some assumptions concerning the properties of the red pools in these two enzymes. Our spectra indicate a similarity of C714 in *Synechocystis* PCC 6803 with C719 in *T. elongatus* and are in agreement with hole-buring experiments also showing a close similarity between C714 and C719 (*18*). Therefore, a strong structural homology of these Chl*a* dimers was concluded (*22*) and is corroborated here. Recently, the emission of C719 was assigned to the dimers A38-A39 and B37-B38, which are close to the reaction center (*29*). Therefore, an assignment of C714 to these dimers is most reasonable. The properties of F699 resemble those observed for C708 of *T. elongatus* (*29*). This pool was assigned to the dimer B7-A32. Therefore, an assignment of F699 to this dimer is also reasonable. The properties of C706 show neither direct equivalence to the single-molecule spectra from *T. elongatus* nor direct equivalence to the single-molecule spectra from *Synechococcus* PCC 7002. The only similarity is the spectral position between the two other pools (F699 and C714). A comparable position between clearly established pools was found in *T. elongatus* for C715. C715 is positioned between C708 and C719. For C715 a very fast spectral diffusion process was proposed. On the basis of this, C715 was assigned to the trimer B31-B32-B33 that shows a composition with high flexibility. This assignment is in agreement with a theoretical study by Vaitekonis et al. (*8*). The reader is referred to this study for a survey of previous theoretical efforts directed toward the assignments of the red pools to Chl*a*s in the structure. It is assumed that the Chl*a* molecule B33 is in an environment likely allowing high flexibility. The *B*-factor of Chl*a* B33 is the largest of this Chl*a* trimer as well as one of the largest within the whole PsaB subunit. Chl*a* B33 is assumed to be missing in PSI from *Synechocystis* PCC 6803[2] (*9*). Absence of the flexible B33 Chl*a* might yield an overall higher rigidity of the remaining dimer and thus to a decrease in the spectral dynamics visible in a higher probability to observe resolved ZPLs in the C706 range in *Synechocystis* PCC 6803.

In summary, the pools F699 (*Synechocystis* PCC 6803), F698 (*Synechococcus* PCC 7002), and C708 (*T. elongatus*) as well as the red-most pools C714 (*Synechocystis* PCC 6803), C708 (*Synechococcus* PCC 7002), and C719 (*T. elongatus*) show similar spectroscopic characteristics on the single-molecule level. This points toward a structural equivalence. It can be suggested that the differences between C706 (*Synechocystis* PCC 6803) and C715 (*T. elongatus*) are due to structural changes of the trimer B31-B32-B33 found in the structure of PSI from *T. elongatus* into the dimer B31-B32 in PSI from *Synechocystis* PCC 6803.

[2] Norbert Krauss, personal communication.

ACKNOWLEDGMENT

We thank Eberhard Schlodder for the PSI samples and for helpful discussion.

REFERENCES

1. Brettel, K. (1997) Electron transfer and arrangement of the redox cofactors in photosystem I. *Biochim. Biophys. Acta 1318*, 322–373.
2. Brettel, K., and Leibl, W. (2001) Electron transfer in photosystem I. *Biochim. Biophys. Acta 1507*, 100–114.
3. Palsson, L. O., Flemming, C., Gobets, B., van Grondelle, R., Dekker, J. P., and Schlodder, E. (1998) Energy transfer and charge separation in photosystem I: P700 oxidation upon selective excitation of the long-wavelength antenna chlorophylls of *Synechococcus elongatus*. *Biophys. J. 74*, 2611–2622.
4. Gobets, B., and van Grondelle, R. (2001) Energy transfer and trapping in photosystem I. *Biochim. Biophys. Acta 1507*, 80–99.
5. Karapetyan, N. V., Schlodder, E., van Grondelle, R., and Dekker, J. P. (2007) *Advances in Photosynthesis and Respiration, Vol. 24, Photosystem I: The Light-Driven Plastocyanin:Ferredoxin Oxidoreductase*, Springer, Berlin.
6. Melkozernov, A. N., Lin, S., and Blankenship, R. E. (2000) Femtosecond transient spectroscopy and excitonic interactions in photosystem I. *J. Phys. Chem. B 104*, 1651–1656.
7. Schlodder, E., Shubin, V. V., El-Mohsnwy, E., Rogner, M., and Karapetyan, N. V. (2007) Steady-state and transient polarized absorption spectroscopy of photosystem I complexes from the cyanobacteria *Arthrospira platensis* and *Thermosynechococcus elongatus*. *Biochim. Biophys. Acta 1767*, 732–741.
8. Vaitekonis, S., Trinkunas, G., and Valkunas, L. (2005) Red chlorophylls in the exciton model of photosystem I. *Photosynth. Res. 86*, 185–201.
9. Sener, M. K., Lu, D. Y., Ritz, T., Park, S., Fromme, P., and Schulten, K. (2002) Robustness and optimality of light harvesting in cyanobacterial photosystem I. *J. Phys. Chem. B 106*, 7948–7960.
10. Gobets, B., van Stokkum, I. H. M., van Mourik, F., Dekker, J. P., and van Grondelle, R. (2003) Excitation wavelength dependence of the uorescence kinetics in photosystem I particles from *Synechocystis* PCC 6803 and *Synechococcus elongatus*. *Biophys. J. 85*, 3883–3898.
11. Byrdin, M., Jordan, P., Krauss, N., Fromme, P., Stehlik, D., and Schlodder, E. (2002) Light harvesting in photosystem I: Modeling based on the 2.5-Angstrom structure of photosystem I from *Synechococcus elongatus*. *Biophys. J. 83*, 433–457.
12. Ben-Shem, A., Frolow, F., and Nelson, N. (2003) Crystal structure of plant photosystem I. *Nature 426*, 630–635.
13. Sener, M. K., Jolley, C., Ben-Shem, A., Fromme, P., Nelson, N., Croce, R., and Schulten, K. (2005) Comparison of the light-harvesting networks of plant and cyanobacterial photosystem I. *Biophys. J. 89*, 1630–1642.
14. Krauss, N., Schubert, W. D., Klukas, O., Fromme, P., Witt, H. T., and Saenger, W. (1996) Photosystem I at 4-Angstrom resolution represents the first structural model of a joint photosynthetic reaction centre and core antenna system. *Nat. Struct. Biol. 3*, 965–973.
15. Jordan, P., Fromme, P., Witt, H. T., Klukas, O., Saenger, W., and Krauss, N. (2001) Three-dimensional structure of cyanobacterial photosystem I at 2.5-Angstrom resolution. *Nature 411*, 909–917.
16. Fromme, P., Jordan, P., and Krauss, N. (2001) Structure of photosystem I. *Biochim. Biophys. Acta 1507*, 5–31.
17. Palsson, L. O., Dekker, J. P., Schlodder, E., Monshouwer, R., and van Grondelle, R. (1996) Polarized site-selective fluorescence spectroscopy of the long-wavelength emitting chlorophylls in isolated photosystem I particles of *Synechococcus elongatus*. *Photosynth. Res. 48*, 239–246.
18. Zazubovich, V., Matsuzaki, S., Johnson, T. W., Hayes, J. M., Chitnis, P. R., and Small, G. J. (2002) Red antenna states of

photosystem I from cyanobacterium *Synechococcus elongatus*: a spectral hole burning study. *Chem. Phys. 275*, 47–59.
19. Elli, A. F., Jelezko, F., Tietz, C., Studier, H., Brecht, M., Bittl, R., and Wrachtrup, J. (2006) Red pool chlorophylls of photosystem I of the cyanobacterium *Thermosynechococcus elongatus*: A single-molecule study. *Biochemistry 45*, 1454–1458.
20. Gobets, B., van Amerongen, H., Monshouwer, R., Kruip, J., Rogner, M., van Grondelle, R., and Dekker, J. P. (1994) Polarized site-selected fluorescence spectroscopy of isolated photosystem-I particles. *Biochim. Biophys. Acta 1188*, 75–85.
21. Ratsep, M., Johnson, T. W., Chitnis, P. R., and Small, G. J. (2000) The red-absorbing chlorophyll a antenna states of photosystem I: A hole-burning study of *Synechocystis* sp. PCC 6803 and its mutants. *J. Phys. Chem. B 104*, 836–847.
22. Hsin, T. M., Zazubovich, V., Hayes, J. M., and Small, G. J. (2004) Red antenna states of PSI of cyanobacteria: Stark effect and interstate energy transfer. *J. Phys. Chem. B 108*, 10515–10521.
23. Hayes, J. M., Matsuzaki, S., Ratsep, M., and Small, G. J. (2000) Red chlorophyll a antenna states of photosystem I of the cyanobacterium *Synechocystis* sp. PCC 6803. *J. Phys. Chem. B 104*, 5625–5633.
24. Frese, R. N., Palacios, M. A., Azzizi, A., van Stokkum, I. H. M., Kruip, J., Rogner, M., Karapetyan, N. V., Schlodder, E., van Grondelle, R., and Dekker, J. P. (2002) Electric field effects on red chlorophylls, beta-carotenes and P700 in cyanobacterial photosystem I complexes. *Biochim. Biophys. Acta 1554*, 180–191.
25. Tamarat, P., Maali, A., Lounis, B., and Orrit, M. (2000) Ten years of single-molecule spectroscopy. *J. Phys. Chem. A 104*, 1–16.
26. Kiraz, A., Ehrl, M., Bräuchle, C., and Zumbusch, A. (2003) Low temperature single molecule spectroscopy using vibronic excitation and dispersed fluorescence detection. *J. Chem. Phys. 118*, 10821–10824.
27. Jankowiak, R., Hayes, J. M., and Small, G. J. (1993) Spectral hole-burning spectroscopy in amorphous molecular-solids and proteins. *Chem. Rev. 93*, 1471–1502.
28. Jelezko, F., Tietz, C., Gerken, U., Wrachtrup, J., and Bittl, R. (2000) Single-molecule spectroscopy on photosystem I pigment-protein complexes. *J. Phys. Chem. B 104*, 8093–8096.
29. Brecht, M., Studier, H., Elli, A. F., Jelezko, F., and Bittl, R. (2007) Assignment of red antenna states in photosystem I from *Thermosynechococcus elongatus* by single molecule spectroscopy. *Biochemistry 46*, 799–806.
30. Brecht, M., Nieder, J. B., Studier, H., Schlodder, E., and Bittl, R. (2008) Red antenna states of photosystem I from *Synechococcus* sp. PCC 7002. *Photosynth. Res. 95*, 155–162.
31. Bautista, J. A., Rappaport, F., Guergova-Kuras, M., Cohen, R. O., Golbeck, J. H., Wang, J. Y., Beal, D., and Diner, B. A. (2005) Biochemical and biophysical characterization of photosystem I from phytoene desaturase and ξ-carotene desaturase deletion mutants of *Synechocystis* sp. PCC 6803. *J. Biol. Chem. 280*, 20030–20041.
32. Müh, F., and Zouni, A. (2005) Extinction coeffcients and critical solubilisation concentrations of photosystems I and II from *Thermosynechococcus elongatus*. *Biochim. Biophys. Acta 1708*, 219–228.
33. Hofmann, C., Aartsma, T. J., Michel, H., and Kohler, J. (2003) Direct observation of tiers in the energy landscape of a chromoprotein: A single-molecule study. *Proc. Natl. Acad. Sci. U.S.A. 100*, 15534–15538.
34. Frauenfelder, H., Sliar, S. G., and Wolynes, P. G. (1991) The energy landscapes and motions of proteins. *Science 254*, 1598–1603.
35. Riley, K. J., Reinot, T., Jankowiak, R., Fromme, P., and Zazubovich, V. (2007) Red antenna states of photosystem I from cyanobacteria *Synechocystis* PCC 6803 and *Thermosynechococcus elongatus*: Single-complex spectroscopy and spectral hole-burning study. *J. Phys. Chem. B 111*, 286–292.

BI800121T